



**HAL**  
open science

## Hybrid laser-ultrasound cavitation for cloud evolution studies

Bjoern Gerold, Spiros Kotopoulos, Sandy Cochran, Michiel Postema, Paul Prentice

► **To cite this version:**

Bjoern Gerold, Spiros Kotopoulos, Sandy Cochran, Michiel Postema, Paul Prentice. Hybrid laser-ultrasound cavitation for cloud evolution studies. *Micro-acoustics in marine and medical research: 1st workshop*, Dec 2011, Bergen, Norway. pp.51-60, 10.5281/zenodo.4779125 . hal-03197833v2

**HAL Id: hal-03197833**

**<https://hal.science/hal-03197833v2>**

Submitted on 21 May 2021

**HAL** is a multi-disciplinary open access archive for the deposit and dissemination of scientific research documents, whether they are published or not. The documents may come from teaching and research institutions in France or abroad, or from public or private research centers.

L'archive ouverte pluridisciplinaire **HAL**, est destinée au dépôt et à la diffusion de documents scientifiques de niveau recherche, publiés ou non, émanant des établissements d'enseignement et de recherche français ou étrangers, des laboratoires publics ou privés.

# 5

## Hybrid laser-ultrasound cavitation for cloud evolution studies

Bjoern Gerold<sup>1</sup>, Spiros Kotopoulos<sup>2</sup>, Sandy Cochran<sup>1</sup>,  
Michiel Postema<sup>2</sup>, Paul Prentice<sup>1</sup>

<sup>1</sup>Institute of Medical Science and Technology (IMSaT), University of Dundee, Dundee DD2  
1FD, UK

<sup>2</sup>Department of Physics and Technology, University of Bergen, Allégaten 55, 5007 Bergen,  
Norway

---

### Abstract

We report on the development of an instrument for hybrid ‘sonoptic’ cavitation studies. A focused ultrasound transducer is housed in a custom-built chamber, which permits optical access to the focal volume, without perturbing the propagating acoustic waves. This configuration allows pulsed-laser irradiation of the liquid at the focus, and simultaneous high-speed observation of cavitation activity in this region. In this paper we provide a brief description of the apparatus and present preliminary data on the distinct cavitation regimes we have observed; specifically, laser-induced cavitation in an established field, and a new phenomenon that we refer to as *laser-nucleated acoustic cavitation*. The former involves a laser-pulse of energy above the threshold value for optical breakdown for the medium, in a pre-established ultrasound field. Here, a cavity rapidly expands to a maximum diameter of a few 100  $\mu\text{ms}$ , from the plasma generated on absorption of the optical energy, and collapses to form debris that is subsequently driven by the ultrasound radiation. By contrast, laser-nucleated acoustic cavitation is initiated by a pulse of *energy below the breakdown threshold*, in a pre-established field. For this regime, either form of radiation does not result in cavitation activity without the

other. In combination, the role of the laser-pulse is to initiate activity which is dominated by the ultrasound exposure from the outset. Crucially, the spatial and temporal precision afforded to the occurrence of cavitation by laser-nucleation, allows us to consolidate our assertion of acoustic cavitation. With observations at unprecedented resolutions, we compare the size of constituent cavities *within a single acoustical cycle* to theoretical predictions, based on the frequency of the ultrasound driving the activity. It is expected that such observations will contribute to a greater understanding of cavitation in focused ultrasound, including for potential future therapeutic applications.

---

## Introduction

### ***Acoustic cavitation***

Acoustic cavitation refers specifically to the formation and subsequent activity of bubbles, or cavities in the pressure fluctuations of an acoustic field, to distinguish from its mechanical or hydro-dynamical counterparts. The phenomenon is a common occurrence in the application of high intensity focused ultrasound (HIFU) fields to the ablation of diseased tissue, known as focused ultrasound surgery (FUS). In this emerging technique, ultrasound is focused transcutaneously to the site of pathology, thus alleviating the need for conventional surgical intervention, and associated risk of infection and extended patient recovery times. In current clinical procedure, the heating is achieved via viscous absorption of the mechanical energy [1], which is most intense at the focus, where the pressure amplitudes are the largest within the field. Heating also occurs in surrounding healthy tissue, such as in the near-field, but at levels that are not harmful, provided the exposure is not prolonged.

Acoustic cavitation occurs in FUS when the rarefactional tension imposed on the tissue during a negative pressure phase, is sufficient to form microscopic cavities, which fill with gas and vapour extracted from the host tissue. The occurrence of the phenomenon depends on a complex mix of the physical properties of the tissue, and the ultrasonic exposure parameters [1]. Continued HIFU excitation acts to further drive the bubble dynamics with a wide range of subsequent physical activity possible, including net growth through rectified diffusion, repulsion due to radiation forces, cloud formation via bubble-bubble interactions (fragmentation and coalescence), and free-radical production or sonochemistry (to mention but a few). It is generally recognized that cavitation in FUS has significant potential to mediate enhanced therapy, such as rapid tissue heating by 'trapping' of the acoustic energy at the focus, or promoting drug delivery via tissue extravasation and microstreaming/pumping [2]. Translation of the phenomenon into medical practice is hampered, in part, by a fundamental lack of understanding of the rapid development of cavitation under HIFU exposure, and parallel development of acoustical detection techniques for monitoring and control purposes. Nonetheless, a growing body of literature demonstrates both active and passive methods of acoustical cavitation detection, and correlation to cavitation related bio-effects in tissue [3], and tissue-mimicking materials [4]. The deficit in understanding cavitation evolution, particularly over the first few hundred acoustic cycles, stem from

several inherent difficulties in studying the phenomenon *in vitro*, including: (1) uncertainty in predicting the exact location within the field, and moment, of cavitation inception, (2) ultra-fast dynamics, driven at the MHz frequencies typical for FUS applications, and (3) cavities in MHz fields tend to be of the order of a few microns. This may be theoretically inferred with the 'rule-of-thumb' simplified *Minnaert's equation* [5], for bubble radius,  $R_f$  resonant to a central ultrasound frequency,  $f_c$ , given by;

$$R_f f_c \approx 3 \text{ ms}^{-1}$$

It may be appreciated that direct observational verification of bubble size is challenging for these reasons. Several studies have attempted to observe and characterize cloud evolution in HIFU fields with high-speed cameras, for example [6]. The best high-speed photography devices available are certainly capable of framing at the Nyquist sampling rate for MHz ultrasound, necessary to fully resolve dynamics. Microscopy objective lenses are also well capable of resolving objects on the micron scale. The researchers were, however, forced to image at spatial and temporal resolutions far below those necessary to make any meaningful observations of cavitation clouds, simply to guarantee the imaging of something! As such, they were restricted to presenting images of 'established' clouds on the millimetre scale, at 10 kHz sampling rates, with little impact on the understanding of the dynamical evolution.

Other researchers have resorted to less direct means for studying cavity sizes in acoustic fields. One such technique relies on sonoluminescence observations in pulsed ultrasound of varying inter-burst durations [7, 8], assuming quiescent bubbles dissolve over a period determined by the initial size. Brothie *et al* [8] developed the technique to report that resonant bubble radii in a 1056 kHz field increase with acoustic power, up to some threshold intensity, at which stage  $R_f$  stabilizes at  $\sim 5 \mu\text{m}$ .

Another approach, based on a similar principle, employed active pulse-receive acoustic detection of bubbles, nucleated via HIFU induced destruction of ultrasound contrast agents (UCAs) [9]. The authors used acoustic scattering to measure resonant dissolution times for 'freed bubbles' in a 1.1 MHz field - at pressure amplitudes similar to those of the present work - by comparing scattering patterns to models adjusted to account for the diffusivities of UCA core gases. Although they had to assume multiple size distributions to fit the data, features from the scattering amplitudes corresponded to  $R_f$ 's  $\approx 0.45, 1.2$  and  $1.56 \mu\text{m}$ .

### ***Laser-induced cavitation***

In contrast to its acoustic counterpart LIC is a very well characterized and understood phenomenon [10], with interest driven largely by ophthalmology applications. This owes to the reliability and reproducibility of employing laser-pulses to generate a cavity at a location, pre-defined by the focal point of a lens, used to concentrate the optical energy into the host medium. LIC studies have contributed greatly to the understanding of

especially single cavity activity, such as jet-formation in the presence of a boundary, and its dependence on the cavity-boundary distance [11]. Although the laser-medium interaction (and to an extent the resulting cavity, such as the degree of asymmetry that evolves) depends somewhat on parameters such as the pulse duration [12], it is well known that the process is plasma-mediated. Absorption of the optical energy at the focus causes localized weak breakdown to form a plasma, which rapidly expands to form a 'hot' cavity of vapour and gas. The requirement for plasma formation imposes an energy threshold on the pulse, below which breakdown does not occur, and a cavity does not form. These factors also translate to a typical lower bound for the maximum diameter LIC bubbles can have, following the initial inflation stage – generally a few 100  $\mu\text{m}$ , with millimetre-sized bubbles being commonly investigated.

In this paper we describe a sonoptic chamber for hybrid laser-acoustic cavitation studies. We use a propagating HIFU field, and introduce cavitation activity by optically focusing a nanosecond laser-pulse into the US focal volume. We have found that reducing the pulse energy to below the breakdown threshold for the system, allows *cavitation nucleation*, without the characteristically large (relative to  $R_f$  determined by the field frequency  $f_c$ ) bubble formation associated with conventional LIC.

## Methodology

The hybrid laser-ultrasound experimental platform has been described in detail elsewhere [13], but a short overview is given here for background. The key feature is the sonoptic chamber that accommodates a HIFU field, the focal region of which can be irradiated with a laser-pulse and observed through a microscope objective lens. We employ a 3 nanosecond frequency-doubled neodymium-doped yttrium aluminium garnet (Nd:YAG) laser-pulse for cavitation induction and nucleation. The pulse is steered into the back aperture of a long working distance objective lens (Mitutoyo 50 $\times$  0.42 NA MPlan NIR  $\infty$ -corrected), from a dichroic mirror reflective to the laser wavelength, 532 nm. The sonoptic chamber is custom-built to 'fit' the HIFU field of a 1.47 MHz focused-bowl transducer, such that the field propagates unhindered by reflection or scattering – other than from cavitation intentionally introduced to the focal region. In this way unwanted interference effects are avoided, and the focused ultrasound may be expected to propagate as it would in an idealised FUS procedure. Fig. 1 (a) depicts the dual focus (optic and ultrasonic) region of the apparatus, schematically. The central glass box is the 'confocal chamber' and contains the liquid which hosts the cavitation activity reported below. The objective lens configuration of fig 1 (a) is that used for the observations reported, whereby one lens focuses the laser and a second orthogonally orientated lens (Mitutoyo 5 $\times$  0.14 NA MPlan APO  $\infty$ -corrected) is used for imaging purposes. This configuration decouples the laser axis from the imaging and allows the laser spot to be translated independently (as distinct from imaging through the focusing lens as described previously [13]). Fig. 1 (b) and (c) depicts the US focus within the confocal chamber, where cavitation is instigated. The transducer is driven by a sinusoid signal from a function generator (Tektronix) passed through an RF power amplifier (Electronics and Innovation) and impedance matching

network. Alignment of the ultrasonic and laser foci is critical to reproducibility, and is achieved through Schlieren imaging to visualise the ultrasound focus, and translation of the chamber to coincide to the laser spot, inset Fig. 1 (a), [14]. Two high-speed cameras were used for the collection of the data presented below, courtesy of the EPSRC instrument loan pool, the Shimadzu HPV-1 and Cordin 550-62. The former is capable of 100 frames at up to 1 Mfps, the latter 62 frames at up to 4 Mfps. The Cordin is a compressed gas-driven rotating drum device, with a formidable reputation. The sensitive optics of the cameras are protected from scattered laser radiation with a green optical filter.

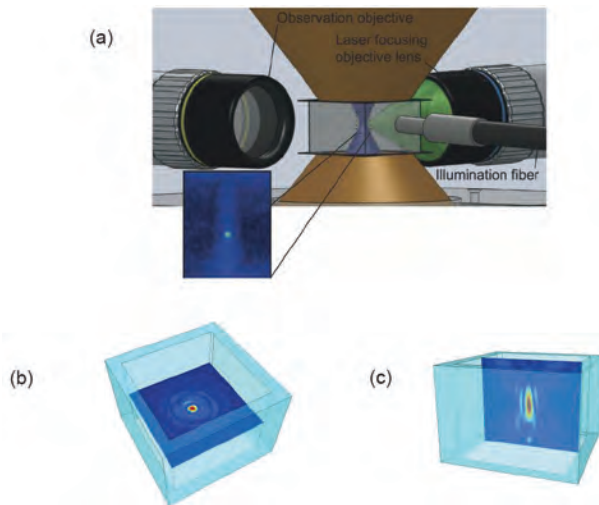


**Figure 1.** Schematic representation of the sonoptic chamber, housing the ultrasound focal volume, and the optical focus of a laser pulse passed through a long working distance microscope objective lens. Inset is a schlieren image of the focal volume (lighter blue) used to align the optical focus (green spot). Simulated, and to-scale representation of the (a) transverse, and (b) axial focus of the HIFU field, within the confocal region of the sonoptic chamber, which has dimensions: 20x20x14mm. Higher peak pressures are indicated red, with ambient atmospheric pressure represented as deeper blue. It can be seen that the chamber housing does not interfere with the propagating pressure field.

Quoted laser-pulse energies are measured at the back aperture of the objective lens with a power meter (ThorLabs), and HIFU peak negative pressure (PNP) amplitudes with a fibre-optic hydrophone (Precision Acoustics). Spatial scales for the high-speed images presented were determined by imaging flow cytometry beads of diameters 10 and 50  $\mu\text{m}$ , *in situ*. For an experiment, the laser is switched to single pulse mode and triggered from the high-speed camera, with an appropriate delay for the Q-switch. The HIFU field is pre-established (turned on) 5-10 seconds before the laser-pulse is generated, and high-speed photography initiated. All the results presented below use degassed (to  $< 4 \text{ mgL}^{-1}$  of dissolved oxygen) tap water as the host medium. The optical breakdown threshold for the system, defined as the pulse energy below which no LIC was observed, was determined to be  $1.10 \pm 0.02 \text{ mJ}$ , where the error is attributed to

instrumental fluctuations in the pulse energies generated, according to the user manual and consistent with our own power meter measurements.

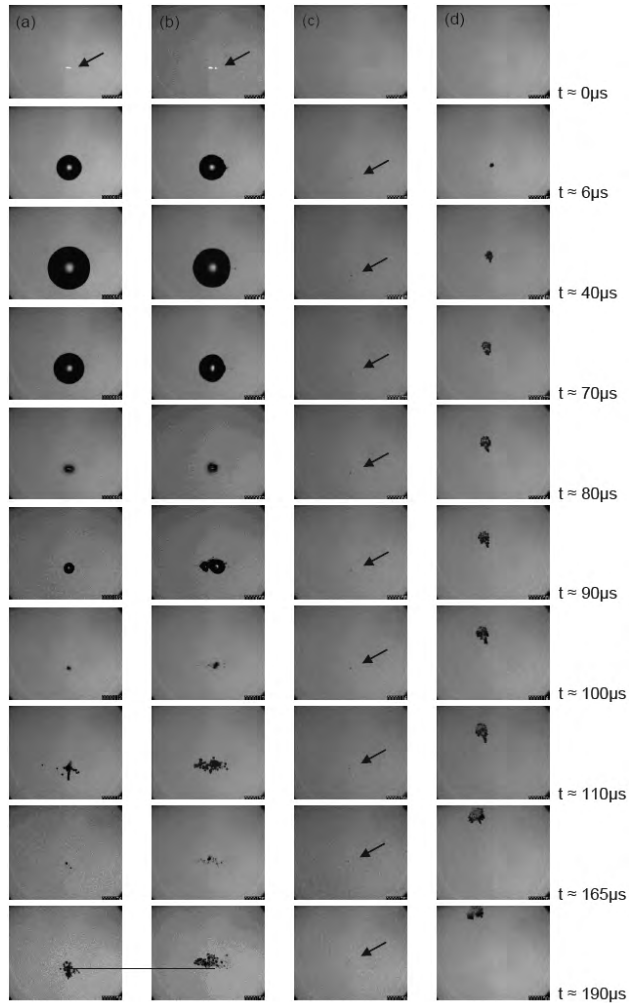


**Figure 2** - Selected individual frames extracted from high speed sequences recorded with the Shimadzu HPV-1 camera operating at 0.5 Mfps ( $\times 10^6$  frames per second), depicting the various regimes of laser-ultrasound cavitation that may be studied with the apparatus: (a) Laser-induced cavitation (LIC) formed with a laser pulse of above the breakdown threshold, (b) LIC in a low intensity ultrasound field. The line across the 190  $\mu$ s images serves to indicate the upwards translation of the debris cloud in the presence of ultrasound. (c) Laser nucleated acoustic cavitation (LNAC) with a laser-pulse below the breakdown threshold, in a low intensity, pre-established ultrasound field, and (d) LNAC in a high intensity, pre-established field. Each frame is 1.2 mm in width.

## Results and Discussion

Fig. 2 (a)-(d) represents the various forms of laser-acoustic cavitation that may be studied with the experimental architecture described. Sequence 2 (a) is representative of conventional LIC, as described in the introductory section above. A  $1.20 \pm 0.02$  mJ pulse is focused into the water, of sufficient energy to cause optical breakdown and plasma formation. A spherical cavity of gas and vapour subsequently expands over  $\sim 40$   $\mu\text{s}$  to a maximum radius,  $R_{\text{max}} \approx 300$   $\mu\text{m}$ . The inertia of the liquid acts to collapse the cavity over the next  $\sim 40$   $\mu\text{s}$ , which then oscillates through a series of rebounds, with a period of  $\sim 20$   $\mu\text{s}$ .

The cavitation debris in the aftermath of the primary LIC is subject to two further stimulations, at  $\sim 110$  and  $\sim 190$   $\mu\text{s}$ . It is well known that plasma formation through the absorption of a laser pulse generates a spherically radiating acoustic transient, as does the collapse of an LIC [10,12]. As the absorption occurs at  $\sim 0$   $\mu\text{s}$  and the collapse at  $\sim 80$   $\mu\text{s}$ , this would imply a propagation time  $\approx 110$   $\mu\text{s}$ , for the each of the transients to return to the site of cavitation. Taking the speed of sound in water as  $1500$   $\text{ms}^{-1}$ , this translates to a total propagation distance of  $\approx 16$  cm. We thereby infer that the transients are reflected, and effectively re-focused, from the spherically curved transducer (of geometric focus 80 mm, see above), as opposed to the walls of the confocal chamber.

Sequence 2 (b) is a recording of the cavitation activity that resulted from a  $1.20 \pm 0.02$  mJ laser-pulse focused into the HIFU field with measured PNP =  $1.3 \pm 0.15$  MPa. The early stages of the dynamics are clearly dominated by LIC, with rapid bubble expansion to an  $R_{\text{max}} \approx 300$   $\mu\text{m}$ , i.e. comparable to that of 2 (a); LIC without ultrasound radiation. The collapse time is also seemingly unaffected by the ultrasound. The only notable differences are the larger volume of cavitation debris and a slight upwards translation ( $\sim 50$   $\mu\text{m}$  at 190  $\mu\text{s}$ , indicated by a line drawn across the images in question, fig. 2) in the centroid of the cloud, in the case of ultrasound radiation being present. We attribute these effects to bubble fragmentation events under the added acoustic energy available to the system, and the action of the primary radiation force [5, 14] (buoyancy is negligible over these timescales, and in any case would act equally in both scenarios).

Sequence 2 (c) captures the cavitation activity resulting from a laser-pulse of  $0.95 \pm 0.02$  mJ incident to the same location as in 2 (b), and in an equivalent field. Such a low energy laser-pulse *does not produce any cavitation activity, without the pre-established US field*. More than fifty tests were undertaken to confirm this. This sequence is representative of the minimal amount of cavitation activity we observed, which consists of a single small nucleus of  $<10$   $\mu\text{m}$  (arrowed black throughout sequence), which proceeds to translate upwards. We term this activity *laser-nucleated acoustic cavitation* (LNAC), to distinguish it from LIC in an established US field, 2 (b).

Note that the translation speed is approximately constant throughout the sequence and commences from the moment of nucleation. This is in contrast to the LIC in the pre-established field, the centroid of which does not notably translate for the first  $\sim 100$   $\mu\text{s}$ . However, the translations speed of the debris cloud of 2 (b) and the LNAC of 2 (c) are comparable, as one would expect in an ultrasound field of equivalent intensity.

Fig. 2 (d) depicts LNAC, again with a laser pulse energy of  $0.95 \pm 0.02$  mJ, incident to the focal volume of a much higher intensity field, of  $\text{PNP} = 4.1 \pm 0.5$  MPa. As for sequence 2 (c), absorption results in a small cavity nucleus that rapidly develops into a cloud of interacting cavities, which translate as a single entity away from the HIFU source. Although the drag may be expected to be greater for this cloud, than for the cavitation of 2 (c), the translation speed is much higher due to the dependence of the radiation force on the square of the pressure amplitude [5,15].

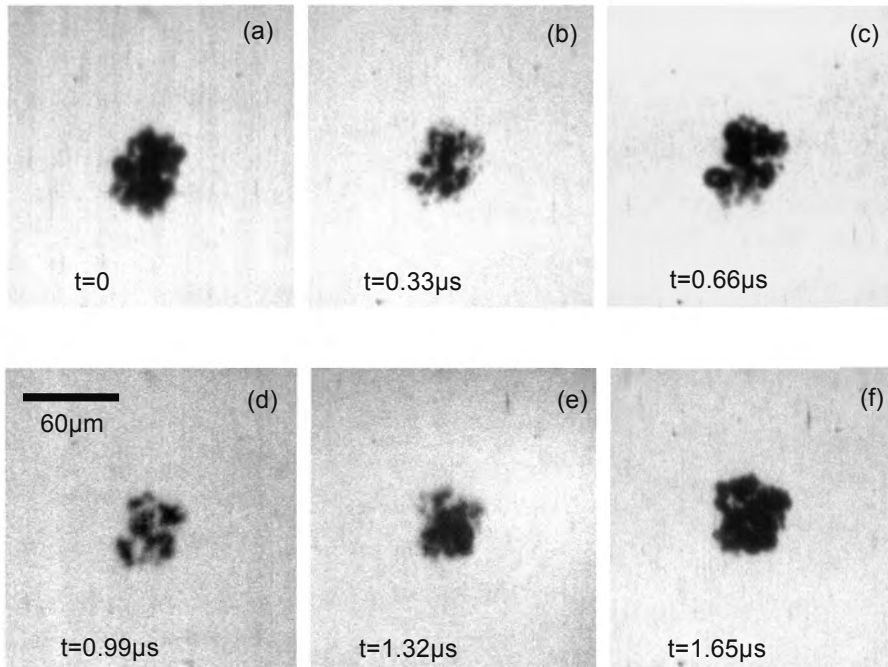


**Figure 3.** Consecutive frames extracted from an ultra high-speed sequence of a LNAC cloud in the early stages of development in an intermediate intensity field. This sequence was recorded at 3.05 Mfps, with timings of each image acquisition as indicated. (a) A cloud of expanded cavities (alternatively, of high 'void fraction', defined as the ratio of gas phase volume to liquid phase volume) indicates a rarefactive negative pressure amplitude phase of the propagating ultrasound in the locale of the cloud. (b) At  $\sim 0.33 \mu\text{s}$  later the cloud appears to be composed of compressed cavities (or is of a lower void fraction) thereby indicating a positive pressure compressional phase of the ultrasound is acting at the time of image acquisition. Note, an  $f_c$  of 1.47 MHz used for this work equates to a pressure phase oscillation period of  $\approx 0.7 \mu\text{s}$ . (c) – (f) Continued cycling under the propagating HIFU pressure fluctuations. Image acquisition was through the 5x objective lens in the orthogonal configuration.

To consolidate our assertion that fig. 2 (c and d) is cavitation that is acoustic in nature, we now consider the size of the component structures within the cloud. In fig. 2 the imaging rate is less than the HIFU frequency, which is adequate to image cloud morphology evolution and translation, but insufficient to resolve component cavity dynamics. The relatively long exposure times used to capture these images result in 'objects' becoming smeared over a region of pixels, as they oscillate under the influence of the incident US. As such, the best we can expect to infer is an upper bound on the maximum diameter during the oscillation. Moreover, this assumes no translation, coalescence, non-symmetrical dynamics etc., which is evidently not the case, and could lead to erroneous measurements.

Fig. 3 (a-f) are close-ups of six consecutive frames extracted from a sequence recorded at 3.05 Mfps, at an 'advanced' stage of LNAC cloud evolution, some 15.8  $\mu\text{s}$  following laser-pulse absorption and initial recorded cavitation activity. This sampling rate satisfies the Nyquist criterion for the 1.47 MHz HIFU frequency used, and as such allows quasi-resolved observation within a single acoustical cycle. Each frame represents an integration of the cavity dynamic over an exposure time significantly less than the inter-frame time of 0.33  $\mu\text{s}$ , compared to the duration of a negative or positive phase of the ultrasound, which at half the period  $\approx$  0.34  $\mu\text{s}$ . The HIFU driving this cavitation was of  $\text{PNP} = 2.20 \pm 0.26$  MPa. This 'mini-sequence' records the cloud through just more than 2 cycles of US propagation. Intuitively, 3 (a)-(c) was recorded during a negative-positive-negative cycle, with (d)-(f) capturing an expansion phase during a negative-positive transition. Fig. 3 (b and d) in particular, allow us to put an upper limit on the minimum radius,  $R_{\text{min}}$ , of some of the cavities within the cloud, of the order of a few  $\mu\text{ms}$ . We estimate that equivalent features in the negative pressure phases of the incident US have  $R_{\text{max}}$ 's in the range of  $\sim 10$   $\mu\text{ms}$ . This would put many of the observable cavities at around the resonant size for the frequency used, in accordance with published literature. We also note that although the apparent translation under the action of the primary radiation force is much reduced from that observed in fig. 2 (d) - due to both reduced US intensity and increased frame rate for sequence acquisition - this might still result in a slight overestimate to the feature dimensions.

## Conclusions

In conclusion, we present preliminary observations on a new technique that allows what appears to be predominantly acoustic cavitation to be nucleated, or seeded, by a nanosecond laser-pulse in an acoustic field. Crucially, the dominance of a large laser-induced bubble is avoided by reducing the pulse energy. The key advantage is the spatial and temporal precision the technique affords, which allows the incorporation of ultra-high speed micro-photography, at the resolutions required to observe cloud formation and evolution.

## Acknowledgements

The research leading to these results has received funding from the European Community's Seventh Framework Programme (FP7/2007-2013) under grant agreement n° 230674 (Nanoporation project).

Paul Prentice acknowledges the Norwegian Research Council for Yggdrasil mobility award no. 210949/F11.

We are particularly grateful to Mr Adrain Walker of the EPSRC instrument loan pool, for continued access to various high-speed imaging devices.

## References

1. ter Haar, G., *Ultrasound focal beam surgery*. Ultrasound Med Biol, 1995. **21**(9): p. 1089-1100.
2. Coussios, C. et al., *Role of acoustic cavitation in the delivery and monitoring of cancer treatment by high-intensity focused ultrasound*. Int J Hyperthermia, 2007. **23**(2): p. 105-120.
3. M<sup>c</sup>Glaughlin, J. et al., *A study of bubble activity generated in ex-vivo tissue by high intensity focused ultrasound*. Ultrasound Med Biol, 2010. **36**(8): p. 1327-1344.
4. Holt, R. and R., Roy, *Measurements of bubble-enhanced heating from focused MHz-frequency ultrasound in a tissue-mimicking material*. Ultrasound Med Biol, 2001. **27**(10): p. 1399-1412.
5. Leighton, T., *Acoustic Bubble*. Academic Press, 1994, London.
6. Chen, H. et al., *High-speed observation of cavitation bubble cloud structures in the focal region of a 1.2 MHz high-intensity focused ultrasound transducer*. Ultrasonics, 2006. **14**: p. 291-297.
7. Lee, J. et al., *Determination of the size distribution of sonoluminescence bubbles in a pulsed acoustic field*. J Am Chem Soc, 2005. **127**: p. 16810-16811.
8. Brotchie, A. et al., *Effect of power and frequency on bubble-size distributions in acoustic cavitation*. Phys Rev Lett, 2009. **102**: p. 084302.
9. Chen, W. et al., *The disappearance of ultrasound contrast microbubbles: observation of bubble dissolution and cavitation nucleation*. Ultrasound Med Biol, 2002. **28**(6): p. 798-803.
10. Fujimoto, J. et al., *Time-resolved studies of Nd:YAG laser-induced breakdown*. Invest. Ophthalmol. Vis. Sci., 1985. **26**: p. 1771-1777.
11. Brujan E. et al., *Dynamics of laser-induced cavitation bubbles near an elastic boundary*. J Fluid Mech, 2001. **433**: p. 251-281.
12. Vogel, A. et al., *Shock wave emission and cavitation bubble formation by picoseconds and nanosecond optical breakdown in water*. J Acoust Soc Am, 1996. **100**(1): p. 148-165.
13. Gerold, B. et al., *Laser-nucleated acoustic cavitation in focused ultrasound*. Rev Sci Inst, 2011. **82**(4): p. 044902.
14. Palanchon, P. et al., *Optical observations of acoustical radiation force effects on individual air bubbles*. IEEE UFFC, 2005. **52**(1): p. 104-110.